Tuberculosis 114 (2019) 77–90

Contents lists available at ScienceDirect

Tuberculosis

journal homepage: www.elsevier.com/locate/tube

Mechanisms of Pathogenesis

Mycobacterium tuberculosis with different virulence reside within intact phagosomes and inhibit phagolysosomal biogenesis in alveolar macrophages of patients with pulmonary tuberculosis

Elena Ufimtseva[a,b,*], Natalya Eremeeva[b], Sergey Bayborodin[c], Tatiana Umpeleva[b], Diana Vakhrusheva[b], Sergey Skornyakov[b]

[a] *Laboratory of Medical Biotechnology, Research Institute of Biochemistry, Federal Research Center of Fundamental and Translational Medicine, 2 Timakova Street, 630117, Novosibirsk, Russia*

[b] *Scientific Department, Ural Research Institute for Phthisiopulmonology, National Medical Research Center of Tuberculosis and Infectious Diseases of Ministry of Health of the Russian Federation, 50 XXII Partsyezda Street, 620039, Yekaterinburg, Russia*

[c] *Shared Center for Microscopic Analysis of Biological Objects, Federal Research Center Institute of Cytology and Genetics, 10 Lavrentyeva Prospect, 630090, Novosibirsk, Russia*

ARTICLE INFO

Keywords:
Mycobacterium tuberculosis
Virulence
Patients with pulmonary tuberculosis
Alveolar macrophages
Phagosomes
Guinea pig

ABSTRACT

Tuberculosis (TB) is a dangerous airborne disease caused by *Mycobacterium tuberculosis* (*Mtb*) and characterized by a tight interplay between pathogen and host cells, mainly alveolar macrophages. Studies of the mechanisms of *Mtb* survival within human cells during TB disease are extremely important for the development of new strategies and drugs for TB treatment. We have used the *ex vivo* cultures of alveolar macrophages and histological sections obtained from the resected lungs of patients with pulmonary TB to establish the unique features of *Mtb* lifestyle in host cells. Our data indicate that *Mtb* with different virulence, as single and in colonies, with or without cording morphology, are exclusively intravacuolar pathogens with intact phagosomal membranes in viable host cells of TB patients and *Mtb*-infected guinea pig. Mycobacteria were detected in the cytoplasm and/or damaged vacuoles only in alveolar macrophages with morphological signs of cell death after prolonged *ex vivo* culture, however *Mtb* were found inside phagosomes in viable alveolar macrophages or cells with apoptotic/necrotic morphology in the same *ex vivo* cell culture. The *Mtb* phagosomes interacted with human different endocytic pathways, but inhibited phagolysosomal biogenesis, while intracellular vesicles containing *Mtb* products were fused with lysosomes in the same host cells.

1. Introduction

Mycobacterium tuberculosis (*Mtb*), the causative agent of tuberculosis (TB), is an extraordinarily successful human pathogen and one of the leading causes of deaths from infectious diseases worldwide [1]. With the increasing prevalence of multidrug resistant and extensively drug resistant *Mtb* [2], there is a need to develop new diagnostics, vaccines and drugs based on the peculiarities of *Mtb*-host interactions in patients with pulmonary TB. As is well known, *Mtb* is spread through aerosols and taken up by alveolar macrophages within the lungs, where the pathogen is typically internalized in the membrane-bound compartment of macrophages and/or dendritic cells, called the *Mtb* phagosome [3–5]. Instead of being eliminated, *Mtb* demonstrates a remarkable ability to survive, replicate, and persist for long periods within human host cells [3–7]. *M. tuberculosis* inhibits phagosomal maturation and blocks delivery to lysosomes through the manipulation of host signal transduction pathways using various strategies and mycobacterial molecules: lipids, such as glycolipid lipoarabinomannan (LAM) and others [3–5,8–10], and proteins, such as the 6-kDa early secretory antigenic target (ESAT-6) protein and the 38-kDa phosphate binding glycoprotein

Abbreviations: Ag38, 38-kDa phosphate binding glycoprotein PstS-1; BAL, bronchoalveolar lavage; BCG, the Bacillus Calmette-Guérin; ESAT-6, 6-kDa early secretory antigenic target; FRET, fluorescence resonance energy transfer; iNOS, inducible Nitric Oxide Synthase; LJ, Lowenstein–Jensen; *Mtb*, *M. tuberculosis*; LAM, lipoarabinomannan; ROS, reactive oxygen species; TB, tuberculosis; ZN, Ziehl-Neelsen

* Corresponding author. Laboratory of Medical Biotechnology, Research Institute of Biochemistry, Federal Research Center of Fundamental and Translational Medicine, 2 Timakova Street, 630117, Novosibirsk, Russia.

E-mail addresses: ufim1@ngs.ru (E. Ufimtseva), eremeevani@yandex.ru (N. Eremeeva), bai@bionet.nsc.ru (S. Bayborodin), tumpeleva@ya.ru (T. Umpeleva), vakhrusheva@urniif.ru (D. Vakhrusheva), sns@urniif.ru (S. Skornyakov).

https://doi.org/10.1016/j.tube.2018.12.002
Received 30 October 2018; Received in revised form 27 November 2018; Accepted 2 December 2018

PstS-1 (Ag38) [5,11]. These *Mtb* products (LAM, ESAT-6, and Ag38) are essential for virulence of *Mtb*, too [12].

In the past decades, several researcher groups have reported that *Mtb* are able to escape from the phagosomal compartment into the cytoplasm of host cells infected in *in vitro* cultures [13–18]. The *Mtb* vacuole-to-cytosol translocation was identified using both electron microscopy techniques [13,14] and the CCF-4 based fluorescence resonance energy transfer (FRET) assay [15–18], which is primarily used to analyze the intracellular localization of Gram-negative bacteria [19]. FRET image analysis of *Mtb* escape from a phagosomal vacuole is based on the constitutive expression of endogenous β-lactamases by *Mtb* naturally resistant to β-lactam antibiotics, such as ampicillin and meropenem [20]. It is also proposed that the β-lactamases of *Mtb* are always membrane-associated proteins located in the cell envelope, β-lactamase activity being presented only on the surface of *Mtb* [15–18]. Consequently, the loading of host cells with a chemical probe, which is a substrate for β-lactamases retained only within the host cytoplasm and sensitive to FRET changes, allows detection of the cytoplasmic contact of *Mtb*, suggesting its phagosomal escape [15–18]. It has been demonstrated that only pathogenic *Mycobacterium* species and patient-derived *Mtb* strains translocate to the cytoplasm of human cells within 1–7 days after *in vitro* infection and that cytoplasmic translocation is an ESAT-6-dependent process and strongly correlates with increased mycobacterial virulence, a more pathogenic phenotype, and cell death induction in human macrophage-like THP-1 cells, monocyte- and bone marrow-derived macrophages [13–18]. It has been proposed that *Mtb* phagosomal rupture and vacuole-to-cytosol translocation are the processes that precede and trigger host cellular death and are required both for *Mtb* replication and dissemination in humans during the development of active pulmonary TB disease [13–18,21,22]. However, other researchers have observed *Mtb* only in the membrane-bound compartments of human macrophages and dendritic cells both infected in *in vitro* culture and isolated from the bronchoalveolar lavage (BAL) fluid of TB patients, with both single and multiple *Mtb* clearly dividing, but the host cells remaining healthy [7,23–25]. Thus, the questions concerning the location of *Mtb* in host cells are not yet answered in full. It is necessary to continue analysis of these fundamental problems in the context of *Mtb*-host cell interactions and the biological significance for *Mtb* survival, replication and virulence, because this knowledge is very important for the development of novel vaccines, therapeutic strategies, and drugs for reduce the burden of TB in the world.

Our interest in these problems arose as early as during the analysis of *Mycobacterium*-host cell relationships in granulomas obtained from various organs of BALB/c mice with latent TB infection caused by *in vivo* exposure to the Bacillus Calmette-Guérin (BCG) vaccine [26]. In those studies, we identified acid-fast BCG mycobacteria actively replicating in some granuloma cells of different types and forming colonies, including those with cording morphology, both within visible membrane-bound vacuoles and without visible membrane structures around replicating microorganisms in large colonies [27]. Also, mouse granuloma macrophages and dendritic cells with from one to up to 100 mycobacteria in each, either as single BCG or as colonies of replicating bacteria, exhibited no morphological signs of cell death and retained their capacity for phagocytosis and disposal of damaged lymphocytes and platelets in *ex vivo* culture [27,28]. On the contrary, throughout days 3–5 following *in vitro* BCG infection, we observed increased death rates of cells heavily loaded with BCG mycobacteria in the cultures of mouse bone marrow and peritoneal macrophages [28,29].

Next, we developed a technique to isolate alveolar macrophages from the resected lung tissues of patients with pulmonary TB [29] and found, in *ex vivo* cell cultures, the presence of a large number of viable alveolar macrophages containing individual *Mtb* or their colonies, including those with cording morphology [30,31]. Also, *Mtb* belonging mainly to the Beijing genotype family in the lungs of the patients studied had different virulence in the guinea pig TB model [31]. Although all the patients received a lot of *anti*-TB drugs in the preoperative period [30], we detected alveolar macrophages with more than 20 highly virulent *Mtb* in each, the host cells being still viable and having neither apoptotic nor necrotic morphology in the *ex vivo* cell cultures from those patients [31].

This situation prompted us to identify the location of *Mtb* in alveolar macrophages obtained from the resected lungs of patients with pulmonary TB and from *Mtb*-infected guinea pig with clinical signs of TB disease. At the first stage, we checked phagosomal integrity by confocal fluorescence microscopy using digitonin (the substance was originally used for analysis of *Francisella*-containing vacuoles [32] and then for detection of *M. marinum* escape from the phagosomes [33]) to label *Mtb* within the cytoplasm and/or disrupted phagosomes in alveolar macrophages of TB patients in *ex vivo* culture. At the second stage, we used light microscopy on the same *ex vivo* cell cultures as on confocal fluorescent images re-stained for acid-fast *Mtb* by the Ziehl-Neelsen (ZN) method [26–29]. Finally, we compared human cells on confocal fluorescent images with the same alveolar macrophages re-stained by the ZN method. Previously, we had used this strategy of re-staining cell preparations for analysis of immunofluorescent labeled CD markers and cytokines versus the content of acid-fast BCG mycobacteria in granuloma cells of mice with latent TB infection [26–29]. Here, the results obtained using the proposed strategy indicate that, after hours 16–18 of *ex vivo* culture, *Mtb* with different virulence, as single and in colonies, including those with cording morphology, were exclusively intravacuolar in the alveolar macrophages of the patients with pulmonary TB and the *Mtb*-infected guinea pig with clinical and histopathological signs of TB disease. Mycobacteria were detected in the cytoplasm and/or damaged vacuoles only in the host cells with morphological signs of cell death after prolonged *ex vivo* culture. However, *Mtb*, as single and in colonies, were found inside phagosomes in viable alveolar macrophages or cells with apoptotic or necrotic morphology in the same *ex vivo* culture of cells. Also, here we describe some characteristics of *Mtb* phagosomes and human intracellular vesicles in cells from the TB patients' lungs. As a result, we demonstrated that the maturation of the *Mtb* phagosomes into phagolysosomes is arrested, but intracellular vesicles containing *Mtb* products are fused with lysosomes in the same host cells. Our findings represent the unique events of *Mtb*-host cell interactions in alveolar macrophages from patients with pulmonary TB and provide further support to the view that *Mtb* is an intravacuolar pathogen able to arrest phagosome maturation and to evade delivery to lysosomes in the TB patients' lung host cells.

2. Materials and methods

2.1. Patients and lung tissue samples

Lung tissue samples were obtained from 26 patients with pulmonary TB at the Department of Thoracic Surgery of the Ural Research Institute for Phthisiopulmonology affiliated with the National Medical Research Center of Tuberculosis and Infectious Diseases of the Ministry of Health of the Russian Federation (Yekaterinburg, Russia) over the period from August 2014 to May 2015 (for patients 1 ÷ 21) and in July 2017 (for patients 22 ÷ 26) as described in Refs. [30,34]. The patients nomenclature used is explained in Ref. [30]. All the patients (age, treatment, attendant diseases, surgery and other parameters) were characterized in detail previously in S1 and S2 Tables in Ref. [30] and here in Table 1. In brief, all the patients had fibrotic and caseotic TB lesions in the lungs and had been referred for the surgical management of treatment-refractory pulmonary TB. A diagnosis of multidrug-resistant TB was established for patients 1, 3, 7 ÷ 12, 14 ÷ 26, and of extensively drug-resistant TB, for patient 6. Seven patients (6 ÷ 10, 22, and 23) had cavities in the lungs. Based on clinical manifestations, chest radiography, and computed tomography (see S2 Table in Ref. [30]) all the patients were divided into three severity groups with different extents of TB disease: “advanced” (patients 6, 7, and 10), “moderate” (patients 5, 8, 15, 16, 20, 22, and 24 ÷ 26), and “minimal” (the others). All procedures

Table 1
The characteristics of patients with pulmonary tuberculosis (TB) and analysis of *M. tuberculosis* (*Mtb*) and alveolar macrophages with *Mtb* obtained from TB patients' resected lungs after surgery.

Patient no.		22	23	24	25	26
Age (years)		55	28	63	42	57
Sex		Male	Male	Male	Male	Male
Diagnosis		MDR TB	MDR TB	MDR TB	MDR TB	MDR TB
Treatment before surgery	Drugs[a]	Z E Pas Cs Of K	H R Z E	Z Pt Cap Pas Cs Lfx	Z Pt Cap Pas Lfx	Z Pt Pas Cs K Lfx
	Months[b]	5	12	7	9	9
Mtb in smear of sputum		–	–	–	–	–
TB lesions	Caseation	+	+	+	+	+
	Fibrosis	+	+	+	+	+
	Macroscopic	cavity	cavity	tuberculoma	tuberculoma	tuberculoma
Surgery[c]	S1-2 RL	S1-2 LL	S1-2 RL	UL RL	S1-2 RL	
HIV infection		–	–	–	–	–
Attendant diseases		–	–	–	–	–
Mtb in smear of tissue homogenate		–	small	small	small	small
Mtb clinic isolate[d]		–	–	–	–	–
Mtb genotype family group		Beijing	Beijing	Beijing B0/W148	Beijing	Beijing B0/W148
TB in guinea pigs		–	–	–	–	–
Mtb virulence		low	low	low	low	low
Lung tissue for processing of alveolar macrophages[e]		distant	distant	tuberculoma	tuberculoma	distant
Macrophages[f] (*n*)		213552	37836	52812	28368	57852
Alveolar macrophages with	*Mtb*[g] (%)	0.12	0.17	3.41	0.76	0.56
	Mtb[h] (*n*)	249	62	1783	214	321
	Mtb in colonies[i] (%)	28.6	–	63.3	16.7	44.4
	Mtb in cords[j] (%)	–	–	29.0	–	25.0
	1 *Mtb*[k] (%)	71.4	100	32.0	83.3	55.6
	2 *Mtb*[k/l] (%)	28.6/100	–	24.0/83.3	–	22.2/100
	3-9 *Mtb*[k/l/m] (%)	–	–	36.0/100/38.9	16.7/100/0	22.2/100/50
	10-20 *Mtb*[k/l/m] (%)	–	–	4.0/100/50	–	–
	> 20 *Mtb*[k/l/m] (%)	–	–	2.0/100/100	–	–

(+), is present; (−), is absent.
[a] H, isoniazid; Z, pyrazinamide; E, ethambutol; Pt, protionamide; Cap, capreomycin; Pas, *para*-aminosalicylic acid; Cs, cycloserine; Of, ofloxacin; K, kanamycin; Lfx, levofloxacin.
[b] Duration of therapy.
[c] S, segment; UL, upper lobe; LL, left lung; RL, right lung.
[d] *Mtb* growth on Lowenstein-Jensen medium.
[e] Distant, lung tissue far from macroscopic TB lesions, tuberculomas, and cavities.
[f] The total number of alveolar macrophages produced from lung tissue sample of TB patient.
[g] Data are presented as percentage of the number of particular cell type out of the total number of examined macrophages stained by the ZN method after *ex vivo* culture for 18 h.
[h] The total number of alveolar macrophages with *Mtb* (single or as colonies) produced from lung tissue sample of TB patient.
[i] Data are presented as the percentage of the number of cells with *Mtb* in colonies out of the total number of macrophages with *Mtb*.
[j] Data are presented as percentage of the number of the cells with *Mtb* cords out of the total number of the macrophages with *Mtb* in colonies.
[k] Data are presented as percentage of the number of the cells with different quantity of *Mtb* (single or as colonies) out of the total number of the macrophages with *Mtb*.
[l] Data are presented as percentage of the number of the cells with *Mtb* in colonies out of the number of the macrophages with corresponding number of *Mtb*.
[m] Data are presented as percentage of the number of the cells with *Mtb* cording out of the total number of the macrophages with *Mtb* in colonies.

involving patients were fully reviewed and approved by the Ethical Committee of the Ural Research Institute for Phthisiopulmonology (27/2014/07/02) and conducted in accordance with the principles expressed in the Helsinki Declaration. Written informed consent was obtained from each patient in this study. Immediately after surgery, pieces of lung tissues (~10–30 g) obtained from lung parts distant from macroscopic TB lesions and cavities were collected for producing alveolar macrophages for patients 1÷5, 7÷23, and 26, pieces of tuberculomas were collected for patients 24 and 25, and the cavity wall of the resected lung was collected for patient 6.

2.2. Ex vivo production of TB patients' alveolar macrophages

Alveolar macrophages from the samples of surgically resected lung tissue of the patients were produced as described in Refs. [30,34]. In brief, samples of lung tissue were cut into small pieces and rubbed through a metal screen of a sieve with pores of 0.5–2.0 mm in diameter in phosphate-buffer saline (PBS, pH 7.4) for separating cellular suspension containing alveolar macrophages from closed granulomatous-fibrotic tissue (see here Figs. S8A–C, F-H). Cellular pellets after centrifugation at 400*g* for 5 min at room temperature were placed to 24-well plates (Orange Scientific, Belgium) with cover glasses in the bottom and cultured in 0.5 ml of RPMI 1640 complete growth medium containing 10% fetal bovine serum, 2 mM glutamine and 50 μg/ml gentamicin (BioloT, Russia) for 16–18 h at +37 °C in an atmosphere containing 5% CO_2. At hours 16–18 of *ex vivo* culture, more than 90% of cells obtained from the cavity wall, tuberculomas, and distant parts of resected lung tissue of all the patients were found to be alveolar macrophages [30]. Besides the alveolar macrophages, five more cell types were observed: dendritic cells, lymphocytes, fibroblasts, neutrophils, and multinucleate Langhans giant cells, but the population sizes of these cells were much lower: see S3 Table in Ref. [30].

2.3. Mtb genotypic classification

An analysis of *Mtb* DNA from the tissue samples obtained from the resected lungs of patients 1÷21 was reported previously in Refs. [30,31]. Here, analysis of *Mtb* DNA from the tissue samples obtained from the resected lung tissues of patients 22÷26 was as described in Ref. [31]. In brief, DNA extraction from the tissue samples obtained from the resected lungs of all the patients was done by using M-Sorb-Tub reagent kits (Syntol, Russia). The DNA obtained was used for PCR

analysis using AmpliTube-RV reagent kits (Syntol, Russia). PCR was performed using a CFX96 analyzer (Bio-Rad, USA). The Beijing and non-Beijing genetic groups were determined by using a real-time PCR Amplitub-Beijing kit (Syntol, Russia). Beijing subgroups were identified using mycobacterial interspersed repetitive unit-variable number tandem repeat (MIRU-VNTR) analysis.

2.4. Evaluation of Mtb virulence in a Guinea pig TB model

The virulence of *Mtb* in the tissue homogenates prepared from the resected lungs of patients 5, 6, 8, and 10 ÷ 21 had previously been detected in guinea pigs in Ref. [31]. Here, the virulence of *Mtb* in the tissue homogenates prepared from the resected lung tissues of patients 22 ÷ 26 was determined in the guinea pigs as described in Ref. [31]. In brief, female outbred guinea pigs were infected by subcutaneous administration of 0.5 ml of the lung tissue homogenates (~5–8 mm^3) in PBS into the right inguinal fold. After infection, the guinea pigs were closely monitored, with particular attention to clinical and morphologic signs of TB disease. After 3 months following TB infection, the animals were euthanized and examined macroscopically and histologically for changes and TB lesions in internal organs. The animal studies were approved by the Ethical Committee of the Ural Research Institute for Phthisiopulmonology (27/2014/07/02). All animal experiments were conducted in accordance with the European Convention for the Protection of Vertebrate Animals used for Experimental and Other Scientific Purposes (ETS no. 123, Strasbourg). As was described in Ref. [31], a high virulence of *Mtb* in the lung tissue homogenates in patients with TB was acknowledged when necrotic TB lesions were detected not only in the lungs, but also in other organs of the guinea pigs; an intermediate virulence of *Mtb* was acknowledged when the homogenized human lung tissue induced TB lesions only in the guinea pig lungs, while a low virulence of *Mtb* was acknowledged if no signs of TB lesions were found in the lungs and other organs of the guinea pigs.

2.5. Guinea pig infection and ex vivo isolation of animal lung cells

A female outbred guinea pig was infected with 0.5 ml of washout from the hands of the nurse in PBS into the right inguinal fold as described in Ref. [35] to determine the degree of *Mtb* contamination in the TB hospital departments and to evaluate the efficiency of infection control measures. At day 79 post infection, the guinea pig with clinical signs of TB disease were euthanized and examined macroscopically and histologically for changes and TB lesions in the right lung, liver, and spleen. Also, the lung piece of this guinea pig was homogenized in PBS and plated on Lowenstein–Jensen (LJ) medium as described in Ref. [31]. After 4 weeks of incubation at +37 °C, mycobacterial colonies were identified and confirmed as being *Mtb* using standard procedures.

Cells were isolated from the left lung of the infected guinea pig following the same procedure as for the alveolar macrophages from the resected lungs of the TB patients and then cultured in 0.5 ml of the complete growth medium under the same conditions as human cells. At hour 20 of *ex vivo* culture, only alveolar macrophages (~80% of the cell population) and polymorphonuclear neutrophils (~20% of the cell population) were observed in the guinea pig cell cultures.

2.6. Differential permeabilization with digitonin

At hours 16–18 of *ex vivo* culture, after removal of growth medium with dead cell debris, monolayer cultures of human and guinea pig cells on the cover slips were washed twice with PBS for removal of non-adherent cells. Further, some human cell cultures were cultured in 0.5 ml of the complete growth medium for 5–7 days at +37 °C in an atmosphere containing 5% CO_2 [36], but the other cell cultures were used for staining with antibodies and other reagents after *ex vivo* culture for 16–18 h. Some of the cell preparations obtained from the resected lungs of patients 5 ÷ 8, 10 ÷ 26 and the guinea pig were incubated with PBS containing 25 μg/ml digitonin (Boehringer Mannheim, Germany, 124672) for 1 min at room temperature and then washed with detergent-free PBS. Macrophages, whose plasma membranes were selectively permeabilized with digitonin or not processed by any detergent, were incubated simultaneously with rabbit polyclonal primary antibodies to *Mycobacteria* LAM (Abcam, England, ab20832) diluted 1:200 to label cytoplasmic mycobacteria and with mouse monoclonal primary antibodies to human Bcl-2 protein (BD Biosciences, USA, 610538) diluted 1:100 to detect delivery antibodies to the macrophage cytoplasm. This procedure was performed in PBS containing 2% BSA for 12 min at room temperature. Macrophages were then washed with PBS and fixed with 4% formaldehyde solution in PBS for 10 min at room temperature. Some of the cell preparations were fixed with 4% formaldehyde solution in PBS for 10 min at room temperature, permeabilized with 0.3% Triton X-100 (triton) for 2 min and stained with the appropriate primary antibodies in PBS containing 2% BSA for 12 min at room temperature. For all cell preparations, bound primary antibodies were visualized with goat polyclonal Alexa 488-conjugated anti-rabbit IgG secondary antibodies (Thermo Fisher Scientific, USA, A11034) and Alexa 555-conjugated secondary antibodies to mouse IgG (Invitrogen, USA, A21422) diluted 1:400 each. The cell preparations were incubated with the secondary antibodies for 60 min at room temperature. Fluorescent staining was analyzed using the VECTASHIELD® Mounting Medium with DAPI (4′,6-diamidino-2-phenylindole) (Vector Laboratories, USA, H-1200). Only for the cell preparations of TB patient 10, alveolar macrophages were incubated for 5 min with the CellMask Orange plasma membrane stain (Invitrogen, USA, C10045) diluted 1:1000 in PBS at +37 °C in 5% CO_2 before permeabilization with different detergents and immunofluorescent staining as described above.

Confocal fluorescent images of human cells were recorded using an LSM 510 or an LSM 780 laser scanning confocal microscope (Zeiss) and the LSM Image Browser or ZEN 2010 software (Zeiss) at the Shared Center for Microscopic Analysis of Biological Objects of the Institute of Cytology and Genetics (Novosibirsk, Russia). Alveolar macrophages were analyzed all along the cells' height by confocal microscopy. The cell preparations incubated with digitonin were washed from VECTASHIELD® Mounting Medium in PBS for 20 min and re-stained for acid-fast *Mtb* by the ZN method. This procedure was only performed on the cell preparations obtained from the resected lungs of the guinea pig and TB patients 6 ÷ 8, 10, and 24 with shares of alveolar macrophages with acid-fast *Mtb* exceeding 1.5% in the *ex vivo* cell cultures, as was previously detected by ZN staining of the other cell preparations in (Ufimtseva et al., 2018a; 2018b) and here. After ZN staining, the cells were further counterstained with Mayer's hematoxylin. Then, alveolar macrophages with acid-fast *Mtb* were viewed using an Axioscop 2 *plus* light microscope. The images of cells were recorded with an AxioCam HRc camera (Zeiss) and analyzed using the AxioVision 4.7 microscopy software (Zeiss). Finally, the cells on the confocal fluorescent images were compared with alveolar macrophages on the ZN images.

The same procedures with digitonin or triton permeabilization, immunofluorescent staining, re-staining for acid-fast *Mtb* by the ZN method, and examination of the cytological preparations were applied to cells obtained from the resected lungs of patients 22 ÷ 24 after *ex vivo* culture for 5–7 days.

2.7. Cell staining to characterize the Mtb phagosomes and host cell vesicles

At hour 18 of *ex vivo* culture, monolayer cultures of human and guinea pig cells on cover slips were washed with PBS and fixed with 4% formaldehyde solution in PBS for 10 min at room temperature. To visualize acid-fast *Mtb* within host cells, some preparations obtained from the resected lungs of patients 22 ÷ 26 and the guinea pig were washed with PBS and stained by the ZN method. After the ZN staining, the cells were further counterstained with Mayer's hematoxylin.

In the experiments using Nile red dye (Invitrogen, USA, N1142), the human and guinea pig cell preparations were incubated with 10 μM of

the dye for 15 min at +37 °C in 5% CO_2 before fixation. The cell preparations were fixed as described above, washed with PBS, blocked in PBS solution containing 2% BSA and 50% bovine serum, and finally incubated first with rabbit polyclonal primary antibodies to *Mycobacteria* LAM (Abcam, England, ab20832) diluted 1:200 (for patients 1 ÷ 21) or ESAT-6 (courtesy of E. V. Deineko of the Institute of Cytology and Genetics, Novosibirsk, Russia [37]) diluted 1:300 (for patients 22 ÷ 26 and the guinea pig), then with Alexa 488-conjugated goat anti-rabbit IgG secondary antibodies (Thermo Fisher Scientific, USA, A11034) diluted 1:400.

In the experiments using LysoTracker Red DND-99 dye (Invitrogen, USA, L7528) or CellROX Deep Red Reagent (Molecular Probes, USA, C10422) with CellEvent Caspase-3/7 Green Detection Reagent (Molecular Probes, USA, C10423), the patients' cell preparations were incubated with 50 nM of the acidotropic dye for 5 min or with 5 μM of reactive oxygen species (ROS) detection dye and 5 μM of caspase-3/7 activation dye for 30 min, respectively, at +37 °C in 5% CO_2 before fixation. The cell preparations were fixed as described above, treated within 2 min in 0.3% Triton-X100 solution (only the cell preparations with LysoTracker dye used), washed with PBS, blocked, and finally stained for *Mycobacteria* LAM as described above.

Some of the patients' fixed cell preparations were washed with PBS, then either blocked and incubated with rabbit monoclonal primary antibodies to human CD14 (Spring Bioscience, USA, M492) or treated within 2 min in 0.3% Triton-X100 solution, blocked and incubated with rabbit polyclonal primary antibodies to human iNOS (Spring Bioscience, USA, E374) diluted 1:100 and mouse monoclonal primary antibodies to the *M. tuberculosis* 38-kDa protein (Abcam, England, ab183165) diluted 1:1000. Fluorescent visualization of CD14 or iNOS and *Mtb* Ag38 was enabled using secondary goat polyclonal DyLight 488- or Alexa 488-conjugated secondary antibodies to rabbit IgG (Thermo Fisher Scientific, USA, 35553 or A11034, respectively) diluted 1:400 and Alexa 555-conjugated secondary antibodies to mouse IgG (Invitrogen, USA, A21422) diluted 1:500.

Some of the patients' fixed cell preparations were washed with PBS, treated for 2 min with 0.3% Triton-X100 solution, blocked, and incubated with Alexa 488-labeled phalloidin (Invitrogen, USA, A12379) or TRITC-labeled phalloidin (Sigma, USA, P1951) dyes diluted 1:200 and 1:100, respectively, to stain filamentous actin for 20 min, and then with rabbit polyclonal primary antibodies to *Mycobacteria* LAM diluted 1:200. Fluorescent visualization of *Mtb* was achieved using goat polyclonal secondary antibodies to rabbit IgG conjugated with DyLight 594 (Thermo Fisher Scientific, USA, 35561) or Alexa 488 diluted 1:400.

The cell preparations were incubated with the appropriate antibodies for 60 min at room temperature. Fluorescent staining was analyzed using the VECTASHIELD® Mounting Medium with DAPI.

The same procedures with immunofluorescent staining were applied to peripheral blood mononuclear cells obtained from three healthy volunteers (Ural Research Institute for Phthisiopulmonology, Yekaterinburg, Russia) and cultured in the complete growth medium under the same conditions as the TB patients' alveolar macrophages. The healthy volunteers gave their written informed consent for the use of their blood for scientific purposes. At hour 18 of *ex vivo* culture, only monocytes (~30% of the cell population) and polymorphonuclear neutrophils (~70% of the cell population) were observed in these cultures on cover slips.

The cytological preparations were examined under the light and laser scanning confocal microscopes as described above. All cells were analyzed separately on each cover slip for each patient in each test. In each cell culture, more than 1000 cells were analyzed.

2.8. Histology

The resected lungs of the TB patients were cut into pieces. One portion of lung pieces was collected for producing alveolar macrophages as described above. The other portion of lung pieces was fixed with 4% formaldehyde solution in PBS (pH 7.4) for 20 h at +4 °C. After fixation, the lung tissues were washed with PBS, incubated with 30% sucrose in PBS (pH 7.4) for 20 h at +4 °C, frozen in Tissue-Tek O.C.T. Compound at −25 °C, and sectioned at 16 μm slides on the Microtome Cryostat HM550 (Microm, Germany) at the Shared Center for Microscopic Analysis of Biological Objects of the Institute of Cytology and Genetics (Novosibirsk, Russia). Sections were air-dried on SuperFrost Plus slides (Thermo Fisher Scientific, USA) and immunofluorescent stained as described above. The histological sections were incubated with the appropriate primary antibodies for 20 h at +4 °C. The histological sections were examined under the LSM 780 laser scanning confocal microscope (Zeiss) as described above. To visualize acid-fast *Mtb* within host cells, sections were stained by the ZN method and further counterstained with Mayer's hematoxylin.

2.9. Statistics

Statistical data processing was performed using MS Excel 2007 (Microsoft). Differences were tested using Student's *t*-test.

3. Results

3.1. M. tuberculosis exhibits unique biological features in alveolar macrophages of TB patients

Using real-time PCR, we assigned *Mtb* in the lung tissue samples from patients 1, 2, 6 ÷ 12, 14 ÷ 20, 22 ÷ 26, and 3, 4 to the Beijing and non-Beijing genotype family groups, respectively (see Table 1 in Ref. [31] and here Table 1). Also, *Mtb* in the lung tissues of patients 6, 10, and 11, 20, 24, 26 were clustered into the A0 and the B0/W148 sublines, respectively. The majority of the patients (without patients 2, 4, 5, and 13) had MDR-TB and XDR-TB (see Table 1 in Ref. [30] and here Table 1). Nevertheless, the number of *Mtb* in the alveolar macrophages of the patients and the number of cells with the different number of *Mtb* (single or as colonies, including those with cording morphology) in them varied significantly between the *ex vivo* cell cultures obtained from the resected lungs of different patients with pulmonary TB after *ex vivo* culture for 16–18 h (see Table 1 in Ref. [31] and here Table 1). In most patients, alveolar macrophages with one and two *Mtb* were found mainly in the *ex vivo* cultures of cells (Fig. 1A–E and Fig. S1C). Alveolar macrophages with more than 2 Mtb, ordinarily in colonies with cording morphology or as irregular clumps, were detected in the *ex vivo* cell cultures obtained from the resected lungs of patients 3 ÷ 10, 14, 17 ÷ 19, and 24 (Fig. 1A–E and Fig. S1B, C). Cords formed by replicating *Mtb* which lined up along their longitudinal axes were identified in alveolar macrophages in one-third of the patients (3, 6, 7, 8, 10, 18, 19, and 24) (Fig. 1A–C and Fig. S1C). All alveolar macrophages with *Mtb* (single or as colonies, including those with cording morphology) or without *Mtb* in them were viable and had neither apoptotic nor necrotic morphology after *ex vivo* culture for 16–18 h (Fig. 1A–E and Figs. S1A-C, S2A). Although *Mtb* in the lung tissue samples from most TB patients were mainly in the Beijing genotype family, they had different potentials to cause TB disease in the guinea pigs, as described earlier in Ref. [31] and here in Table 1. Finally, distinct *Mtb* virulence patterns were discriminated in the guinea pig TB model: *Mtb* from the lung tissue homogenates of patients 6, 8, 10, and 20 were highly virulent; *Mtb* from the lung tissue of patient 18 displayed an intermediate level of virulence; *Mtb* from the resected lungs of patients 5, 11 ÷ 17, 19, and 21 ÷ 26 had low virulence.

3.2. M. tuberculosis resides within intact phagosomes in TB patients' alveolar macrophages

To determine the intracellular location of *Mtb* in the alveolar macrophages of patients with pulmonary TB (5 ÷ 8 and 10 ÷ 26, $n = 21$) after *ex vivo* culture for 16–18 h, we checked phagosomal integrity by

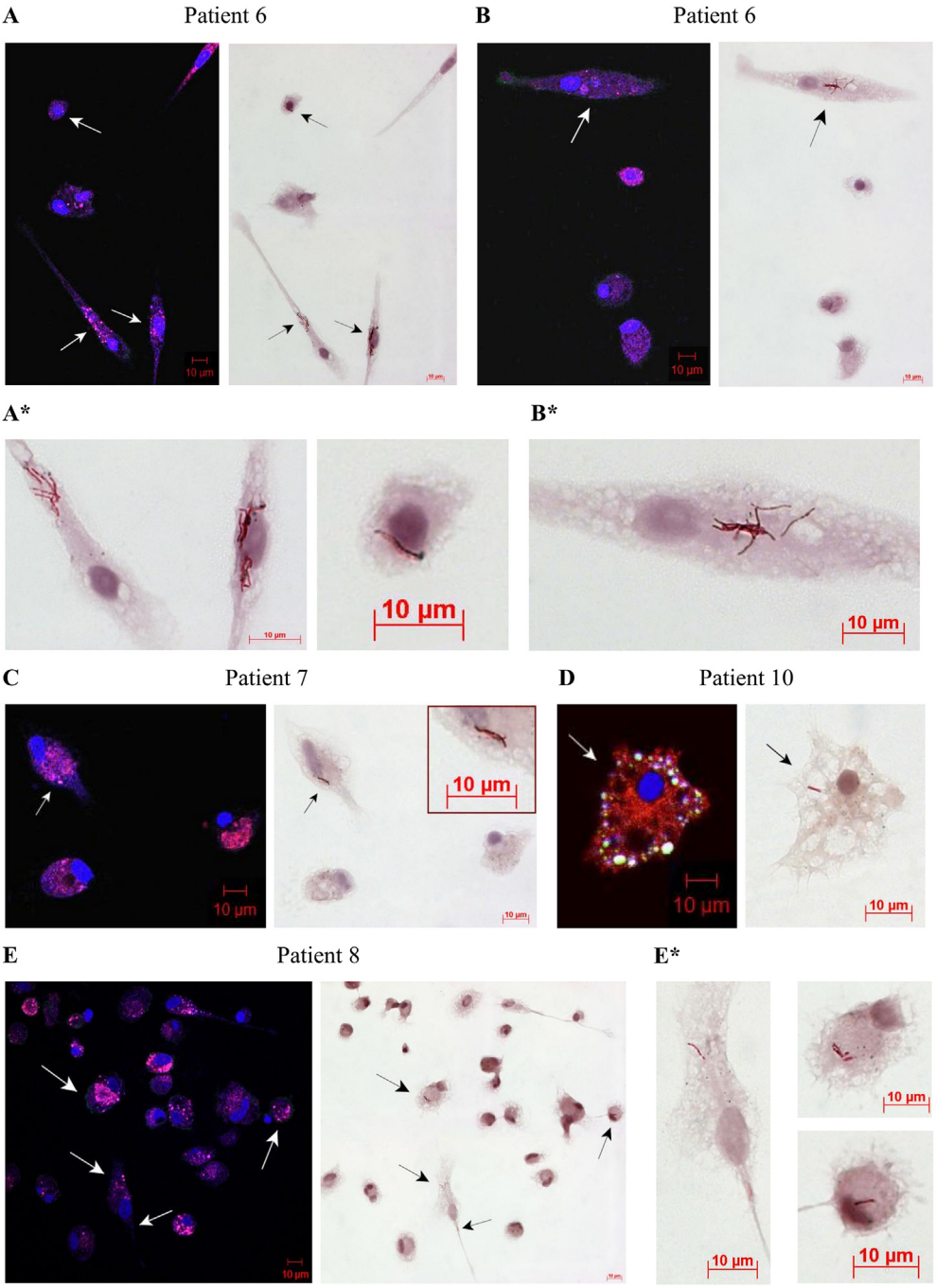

Fig. 1. Mycobacteria reside inside phagosomes in alveolar macrophages obtained from the resected lungs of patients with pulmonary TB. (A–E) In the left panels: immunofluorescent staining of the TB patients' alveolar macrophages by antibodies reacting with *Mtb* LAM (green signal) and Bcl-2 protein (red signal) after permeabilization with digitonin identifies Bcl-2 protein and reveals the lack of *Mtb* in the cytoplasm of human cells analyzed after *ex vivo* culture for 16–18 h. Nuclei are stained by DAPI (blue signal). In the right panels: the same fragments as in the left panels re-stained for acid-fast *Mtb* by the ZN method. Acid-fast *Mtb*, as (D, E) single and (A-C, E) in colonies, including (A–C) some with cording morphology, are determined in the same alveolar macrophages without *Mtb* LAM staining that are shown in the left panels and indicated by the white arrows on the confocal fluorescent images and the black arrows on the ZN images. (A*, B*, E*) Close-ups of the parts of these images that contain alveolar macrophages infected with *Mtb*. (C) Close-ups of the part of this image with *Mtb* cording are in the upper right corner. (D) Fluorescent staining of an alveolar macrophage by the CellMask Orange plasma membrane stain. The images are representative. The scale bars are 10 μm each. (For interpretation of the references to colour in this figure legend, the reader is referred to the Web version of this article.)

confocal fluorescence microscopy, using digitonin and Triton X-100 (triton) to differentially label *Mtb* that are cytoplasmic or within a damaged phagosomes and those enclosed within intact phagosomes. Next, we re-stained the cell preparations incubated with digitonin for acid-fast *Mtb* by the ZN method and compared the confocal fluorescent and the ZN images of the same areas to determine *Mtb*-containing host cells. As is known [32,33], digitonin is a mild nonionic detergent which permeabilizes only macrophage plasma membranes, while leaving phagosomal membranes intact, but triton solubilizes phagosome membranes as well as plasma membranes. Following permeabilization with digitonin or triton, alveolar macrophages were incubated simultaneously with the antibodies to the major *Mtb* cell wall component glycolipid lipoarabinomannan (LAM) to detect cytosolic mycobacteria and/or microbes in damaged vacuoles and to human Bcl-2 protein to detect delivery of antibodies to the macrophage cytoplasm. The analysis of the Bcl-2 protein in human cells was employed, because we had previously determined a higher amount of this protein in the majority of granuloma macrophages, with or without BCG mycobacteria in them, obtained from mice with granulomatous TB inflammatory regions in the different organs of animals, and their colocalization with mitochondria [29]. As is known, the Bcl-2 protein located in the outer mitochondrial membrane is one of the main factors that maintain mitochondrial membrane integrity and protect cells from apoptosis [38,39]. The contribution of the Bcl-2 protein to the survival of TB patients' alveolar macrophages will be discussed in detail in another article. Here, the use of Bcl-2 protein staining allowed us to detect digitonin-permeabilized human cells (Fig. 1A–E and Fig. S1A, B).

In all the patients, a very small amount of *Mtb* LAM and Bcl-2 protein was labeled in the absence of cytoplasmic delivery of the antibodies in the cells not exposed to detergents – this weak staining may

be caused by endocytosis of primary antibodies by living cells (Fig. S1A). Only the Bcl-2 protein was identified in the cytoplasm of human cells after differential permeabilization of macrophage membranes by digitonin (Fig. 1A–E and Fig. S1A), but *Mtb* LAM and Bcl-2 were found in the TB patients' cells permeabilized with triton (Fig. S1A and C). Remarkably, no LAM-stained *Mtb* were detected in digitonin-incubated cells of patient 6 (Fig. 1A and B), although the largest number of infected alveolar macrophages (up to 38% of the cells examined) was found in the *ex vivo* culture of cells obtained from the cavity wall of this patient's lung (see S4 Table in Ref. [30]). Note that LAM-labeled *Mtb* on the cell preparations permeabilized with digitonin were detected only outside the cytoplasm of human alveolar macrophages (Fig. S1B). On the ZN-re-stained cell preparations from patients 6 ÷ 8, 10, and 24, acid-fast *Mtb*, as single and in colonies, including those with cording morphology, were recognized in the alveolar macrophages that had not stained for *Mtb* LAM after digitonin permeabilization (Fig. 1A–E), suggesting the presence of *Mtb* in membrane-bound phagosomes. Moreover, both *Mtb* in colonies with a large number of microbes and a few *Mtb* detected in the different parts of the same host cells were found as located only inside phagosomes with intact membranes in the TB patients' alveolar macrophages (Fig. 1A, B, and E). Noteworthy, the alveolar macrophages were obtained from resected lung tissues with different TB lesions: the cavity wall in patient 6, tuberculomas in patients 24 and 25, and lung parts distant from macroscopic TB lesions and cavities in the others patients. Furthermore, distinct *Mtb* virulence patterns were discriminated in the guinea pig TB model: increased virulence in the resected lungs of patients 6, 8, 10, 18, and 20, and low virulence in the lung tissues of other patients.

Thus, after hours 16–18 of *ex vivo* culture, *Mtb* with both high and low virulence, as single and in large colonies, including those with cording morphology, were exclusively intravacuolar pathogens in alveolar macrophages obtained from different TB lesions in the resected lungs of all the patients with pulmonary TB.

3.3. *M. tuberculosis are located in the cytoplasm and/or damaged vacuoles in some apoptotic/necrotic host cells*

Some of the cell cultures obtained from the resected lungs of patients 22, 23, and 24 were cultured simultaneously in the same complete growth medium under the same conditions for 5–7 days, as described in Ref. [36]. After hours 18 of *ex vivo* culture, only viable cells were determined in the cell cultures from these patients (Fig. S2A). After prolonged *ex vivo* culture, we found the largest number of alveolar macrophages with morphological signs of cell death (nuclei with intense chromatin condensation, nuclear fragmentation, compromised cytoplasmic membranes, leakage of cell components, the occurrence of nucleus-free cells and chromatolysis), both with and without *Mtb* in them, in all cell cultures from patient 24 (Fig. 2B–G and Fig. S2A, B), while only live alveolar macrophages were found in the cell cultures from the other patients (Fig. S2A). Note that neither the population of infected alveolar macrophages nor the *Mtb* populations in host cells changed in these cell cultures from any of these patients after prolonged *ex vivo* culture (Fig. 2A). The virulence of *Mtb* in the lung tissue samples from these patients was characterized as low. After *ex vivo* culture for 5–7 days and the use of the same procedures with digitonin or triton permeabilization and immunofluorescent *Mtb* LAM and Bcl-2 protein staining and re-staining for acid-fast *Mtb* by the ZN method, *Mtb* LAM was detected only in the host cells permeabilized with triton on the cell preparations from patients 22 and 23. However, we revealed *Mtb* LAM staining in alveolar macrophages after both digitonin (Fig. 2A and E-G) and triton (Fig. 2H) permeabilization in the cell cultures from patient 24. Notably, all these *Mtb* LAM-stained host cells incubated with digitonin had apoptotic or necrotic morphology (Fig. 2E–G). In addition, on the same cell preparation re-stained by the ZN method, acid-fast *Mtb*, as single and in colonies, including those with cording morphology, were detected in the same alveolar macrophages, both with lack of *Mtb* LAM staining (Fig. 2B–D) and with *Mtb* LAM staining (Fig. 2E–G), which was indicative of the presence of *Mtb* both inside phagosomes with intact membranes in viable (Fig. 2B and C) or apoptotic/necrotic (Fig. 2D) host cells and in the cytoplasm and/or damaged vacuoles in alveolar macrophages only with morphological signs of cell death (Fig. 2E–G). Interestingly, few host cells with apoptotic/necrotic morphology and *Mtb* LAM staining were detected in the cell culture without the use of detergents (Fig. 2A). Noteworthy, the Bcl-2 protein staining was observed in a lower number of alveolar macrophages from patient 24 after *ex vivo* culture both for 18 h and 5 days (Fig. 2B–H and Fig. S1C), but Bcl-2 was found in the majority of alveolar macrophages from patients 22 and 23 at different times of *ex vivo* culture (Fig. S1A).

Thus, *Mtb* were detected in the cytoplasm and/or damaged vacuoles only in host cells with morphological signs of cell death after prolonged *ex vivo* culture. However, *Mtb*, as single and in colonies, including those with cording morphology, were found inside phagosomes in viable alveolar macrophages and some host cells with apoptotic or necrotic morphology in the same *ex vivo* culture of cells. Therefore, the death of many alveolar macrophages, with and without *Mtb* in them, for unknown reasons in the all the cell cultures from patient 24 after prolonged *ex vivo* culture was a preliminary to damaging the phagosome membranes and then, probably, to *Mtb* vacuole-to-cytosol translocation.

3.4. *M. tuberculosis is an intravacuolar pathogen in Guinea pig cells*

Using the same procedures with permeabilization with different detergents, immunofluorescent *Mtb* LAM and Bcl-2 protein staining and re-staining for acid-fast *Mtb* by the ZN method, we characterized *Mtb* localization in the departments of host cells obtained from the lung of a guinea pig with clinical signs of TB disease after *ex vivo* culture for 20 h. The guinea pig was infected in a special study to assess the efficiency of infection control measures in TB hospital departments [35]. The macroscopic and histological examination identified TB lesions in the different organs of the guinea pig, including the lung (Fig. 3A). Mycobacteria from a lung tissue sample of this animal were clustered to the *M. tuberculosis* of the Beijing genotype family (B0/W148 cluster). In the *ex vivo* cell culture obtained from the lung of this guinea pig, we detected 0.72% of alveolar macrophages and 1.29% of neutrophils with one, two or three acid-fast *Mtb* in each, either as single or as replicating microbes (Fig. 3B). All alveolar macrophages and neutrophils, with or without *Mtb* in them, were viable and had neither apoptotic nor necrotic morphology (Fig. 3B and C). The lack of *Mtb* LAM staining in the cytoplasm of animal cells both permeabilized with digitonin and without the use of any detergent, the *Mtb* LAM staining in guinea pig cells with triton permeabilization, and the identification of acid-fast *Mtb* in animal cells incubated with digitonin and then re-stained by the ZN method demonstrated the presence of *Mtb* in intact phagosomes (Fig. 3C). Bcl-2 protein staining in the guinea pig' cells was not observed in any of the cell cultures (Fig. 3C). According to the Technical Data Sheet (BD Biosciences), the primary antibodies used identify the Bcl-2 protein in human, chicken, dog, mouse, rabbit, and rat cells, but are very unlikely to detect the guinea pig Bcl-2 protein.

On the whole, our study established the exclusively phagosomal localization of *Mtb* in viable host cells of patients with pulmonary TB and *Mtb*-infected guinea pig with clinical and histopathological signs of TB disease.

3.5. *Characteristics of the Mtb phagosomes and human intracellular vesicles in TB patients' alveolar macrophages*

After establishing the phagosomal localization of *Mtb*, we studied *Mtb*-containing vacuoles in human host cells after *ex vivo* culture for 16–18 h. In a confocal fluorescence microscopy assay using different antibodies and other reagents, the colocalization of the receptor CD14 with all the *Mtb* phagosomes in the patients' host cells was revealed (Fig. 4A and Fig. S3A). At the same time, we identified some quantity of

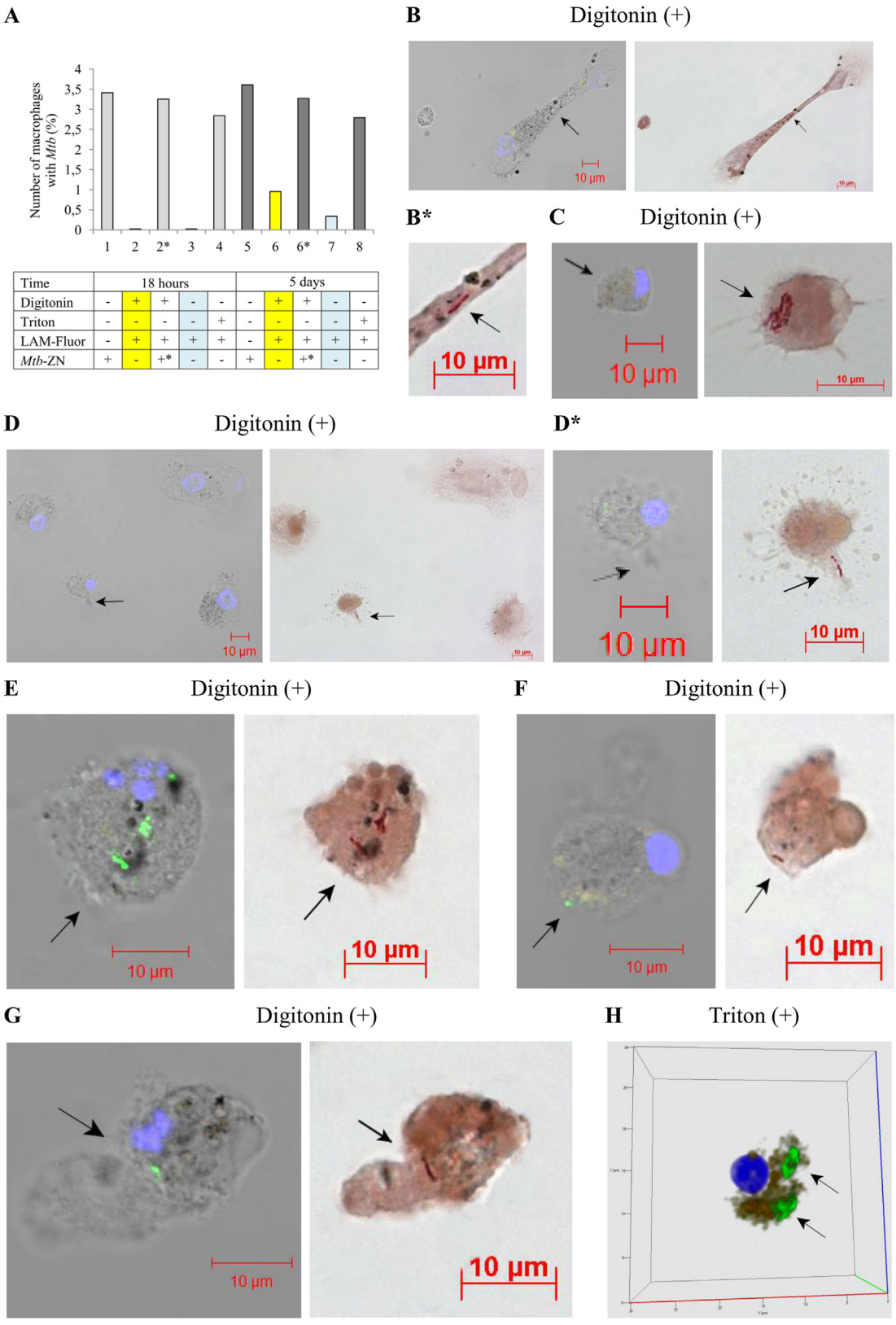

Time	18 hours					5 days				
Digitonin	-	+	+	-	-	-	+	+	-	-
Triton	-	-	-	-	+	-	-	-	-	+
LAM-Fluor	-	+	+	+	+	-	+	+	+	+
Mtb-ZN	+	-	+*	-	-	+	-	+*	-	-

(caption on next page)

ROS and iNOS in many vacuoles containing both single mycobacteria and *Mtb* in colonies, including those with cording morphology (Fig. 4B, C, and Figs. S4A, S5A, B). As is known, the various forms of ROS and nitric oxide produced by iNOS are efficient antimicrobial agents which can damage proteins, lipids, and DNA of pathogens in phagosomes [5]. Note that no ROS or iNOS were detected in some *Mtb* phagosomes in other host cells of the same TB patients (Figs. S4A and S5C). Also, some *Mtb* phagosomes colocalized with lipids (Fig. S6A), but no lipids were found in the other *Mtb*-containing vacuoles, including those with cording morphology, in the alveolar macrophages of the same TB

Fig. 2. Mycobacteria reside both (B–D) inside phagosomes and (E–G) in the cytoplasm and/or damaged vacuoles in TB patient' alveolar macrophages with apoptotic/necrotic morphology. (A) The number of alveolar macrophages with *Mtb* (as single or as colonies) in the cell cultures obtained from the resected lung of patient 24 and incubated with/without different detergents, and after immunofluorescent (Fluor) or/and ZN staining is expressed as the percentage of the total number of macrophages in them after *ex vivo* culture for different periods of time. The *x* axis represents the *ex vivo* cultures of cells with (+) or without (−) permeabilization with different detergents and after some staining. *Analysis was performed in the cell cultures re-stained for acid-fast *Mtb* by the ZN method. (B-G, D*) In the left panels: phase-contrasted confocal fluorescent images of alveolar macrophages (after prolonged *ex vivo* culture) stained by antibodies reacting with *Mtb* LAM (green signal) and Bcl-2 protein (red signal) after digitonin permeabilization. In the right panels: the same fragments as in the left panels re-stained for acid-fast *Mtb* by the ZN method. The scale bars are 10 μm each. (B-D, D*) In the right panels: acid-fast *Mtb*, as (B, D) single and (C) as a colony with cording morphology determined in the same alveolar macrophages without *Mtb* LAM staining, both (B, C) viable and (D, D*) with the signs of cell death, that are shown in the left panels and indicated by the black arrows on the confocal fluorescent and ZN images. (B*, D*) Close-ups of the parts of these images that contain alveolar macrophages infected with *Mtb*. (E–G) Mycobacteria, as (E–G) single and (E) as a colony, detected in the cytoplasm and/or damaged vacuoles only in host cells with morphological signs of cell death. (H) An immunofluorescent confocal 3D image shows a viable alveolar macrophage with two *Mtb* cording structures and Bcl-2 protein staining after permeabilization with triton. (B-H, D*) Nuclei are stained by DAPI (blue signal). (For interpretation of the references to colour in this figure legend, the reader is referred to the Web version of this article.)

patients and guinea pig (Fig. 4D and Fig. S6B). Although ROS-, iNOS-, and Nile red-positive cells were not found in peripheral blood mononuclear cell cultures isolated from healthy human donors and *ex vivo* cultured in the same complete growth medium under the same conditions as TB patients' alveolar macrophages (data not shown), we identified different numbers of ROS-, iNOS- and Nile red-positive alveolar macrophages, with or without *Mtb*, in the *ex vivo* cultures of cells obtained from the resected lungs of each TB patient (Fig. 5A). No statistically significant changes in these parameters were found between the groups of patients with different extents of TB disease (Fig. 5B). We did not observe activation of caspase 3/7 in human host cells with *Mtb*, as single or in colonies, with or without cording morphology, or in cells without *Mtb* (Fig. 4B and Fig. S4A, B). Additionally, we revealed numerous intracellular vesicles containing *Mtb* products (Ag38, ESAT-6, or LAM) and, often together with them, the receptor CD14, ROS, iNOS, and lipids in the TB patients' alveolar macrophages and multinucleate Langhans giant cells, with or without *Mtb* in them, in all *ex vivo* cell cultures both with the largest number of infected host cells (for example, in patients 6, 7, 9 (Fig. S6A), and 24 (Fig. 4A–D and Figs. S4A, S5D, S6B) with 37.72%, 3.04%, 6.54%, and 3.41% *Mtb*-infected cells, respectively) and with a very low number of *Mtb*-containing alveolar macrophages (for example, in patients 4 (Fig. S6A), 14 (Figs. S3A, B, and S5A), 15 (Fig. S5A), 19 (Figs. S3A and S5C, D), 22 (Figs. S4A, B, S5D, and S6C), 25 (Figs. S3A, B, S4B, S5D, and S6C), and 26 with 0.56%, 0.36%, 0.47%, 0.15%, 0.12%, 0.76%, and 0.56% *Mtb*-infected cells, respectively (see S4 Table in Ref. [30] and here Table 1)). Also, these vesicles were stained by DAPI dye (Figs. S3A, B, S4A, B, S5A-D, and S6A-C) which labels mostly DNA, but may also stain RNA. Different *Mtb* products (Ag38 and ESAT-6) were localized in the same human intracellular vesicles (Fig. 6C). The markers examined were also found on the cell surface of alveolar macrophages and multinucleate Langhans giant cells (Figs. S3B and S5D). Probably, intracellular vesicles transported cargo to the cell surface, after which the antigens were secreted by human cells. Noteworthy, no LAM-stained vesicles were detected in digitonin-incubated cells (Figs. 1A–E, 2B-G, and Fig. S1A, B), and so human intracellular vesicles were surrounded by intact membranes.

Mycobacterial antigens (Ag 38, ESAT-6, and LAM) and the human receptor CD14, iNOS, Bcl-2 protein, and lipids were also detected in the many human alveolar macrophages and multinucleate Langhans giant cells on the histological sections from the resected lungs of the TB patients (for example, the patients 10 (Fig. S7A–F) and 24 (Fig. S7G-L)). We revealed the colocalization of *Mtb* products with human markers in a large number of vesicles in alveolar macrophages on the histological sections (Fig. S7A-L), but *Mtb*-infected cells were rare both in the *ex vivo*

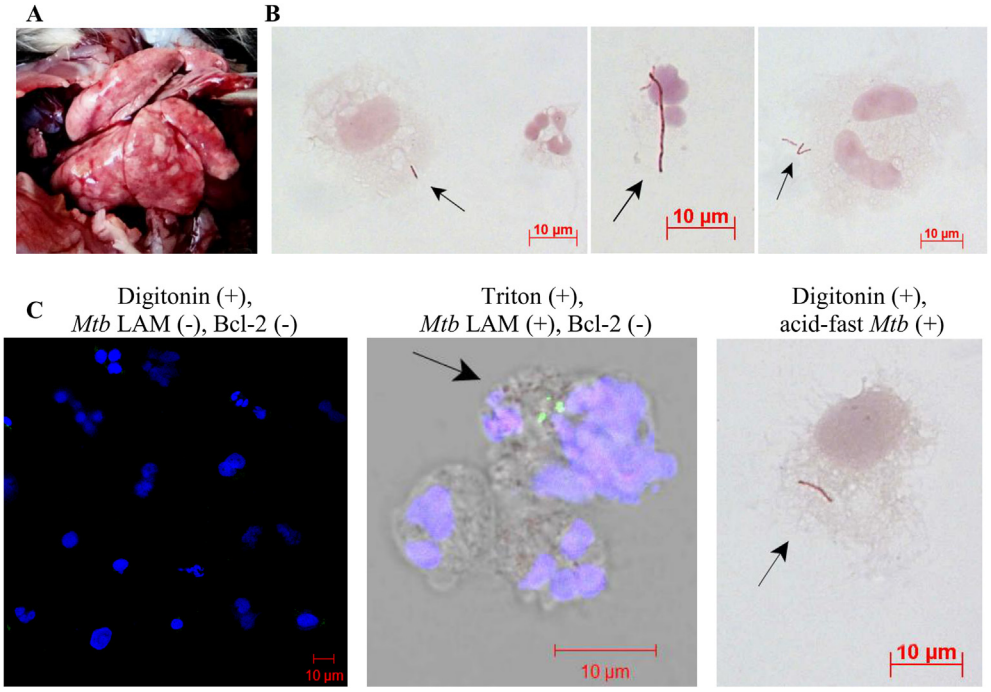

Fig. 3. Mycobacteria localize within vacuoles in host cells obtained from the lung of *Mtb*-infected guinea pig. (A) The lungs of the guinea pig with clearly visible caseous TB lesions. (B) Acid-fast *Mtb* (as single or as colonies) after ZN staining are observed in (left and right panels) alveolar macrophages and (central panel) neutrophil. (C) Immunofluorescent staining of guinea pig cells by antibodies reacting with *Mtb* LAM (green signal) and Bcl-2 protein (red signal) reveals (left panel) the lack of *Mtb* LAM and Bcl-2 protein staining in the cytoplasm of cells permeabilized with digitonin and (central panel) LAM-labeled *Mtb* inside a neutrophil in a cell preparation incubated with triton. Nuclei are stained by DAPI (blue signal). In the central panel: a phase-contrasted confocal image. In the right panel: acid-fast *Mtb* determined in an alveolar macrophage in the same cell preparation that had previously been incubated with digitonin, immunofluorescent stained and analyzed by confocal microscopy, with no *Mtb* detected, and then re-stained by the ZN method. (B, C) Representative images of cells analyzed after *ex vivo* culture for 20 h. The scale bars are 10 μm each. (For interpretation of the references to colour in this figure legend, the reader is referred to the Web version of this article.)

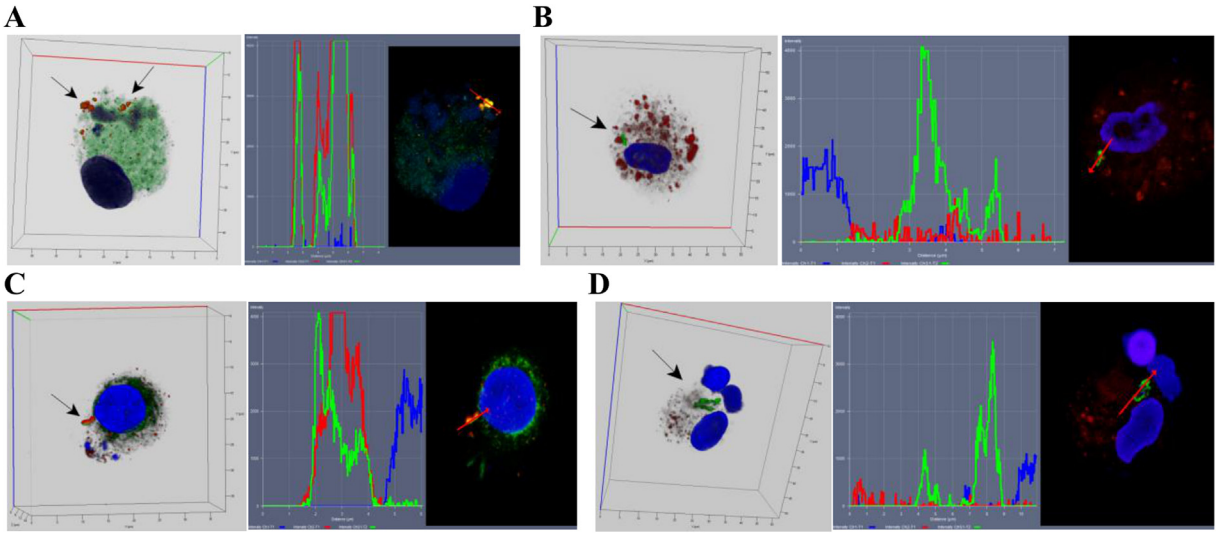

Fig. 4. *M. tuberculosis* cord-containing vacuoles are characterized by different phagosomal sings in alveolar macrophages of patient 24 after *ex vivo* culture for 18 h. (A–D) Representative confocal fluorescent images of cells stained by antibodies reacting with *Mtb* Ag38 (red signal in (A, C)), *Mtb* LAM (green signal in the cytoplasm in (B)), *Mtb* ESAT-6 (green signal in (D)), CD14 (green signal in (A)), iNOS (green signal in (C)) and the CellEvent Caspase-3/7 Green Detection Reagent (green signal in a nucleus in (B)), the CellROX Deep Red Reagent (red signal in (B)), the Nile red dye (red signal in (D)) demonstrate colocalization of *Mtb* antigens with CD14, some ROS, and iNOS (yellow signals) in (A, B, C, respectively) the *Mtb* phagosomes, but show lack of colocalization of *Mtb* cord with lipids (lack of yellow signal) in (D) the *Mtb* phagosome and lack of active caspase-3/7 (lack of green signal in a nucleus) in (B). Nuclei are stained by DAPI (blue signal). Black arrows point to *Mtb* cords on confocal 3D images of host cells. To the right of 3D images: the profile images of the *Mtb* phagosomes in these cells. Red arrows identify the areas for construction of profile images. (For interpretation of the references to colour in this figure legend, the reader is referred to the Web version of this article.)

cell cultures (see S4 Table in Ref. [30] and here Table 1) and on the histological sections of most TB patients (Figs. S7D and J, and S8A-J).

Thus, the TB patients' alveolar macrophages had been producing ROS and iNOS, and so these macrophages had increased microbicidal potential, but contained individual and replicating *Mtb* in membrane-bound intact phagosomes with the same characteristics as human intracellular vesicles.

3.6. *M. tuberculosis arrests phagolysosomal maturation in alveolar macrophages of TB patients*

No colocalization of the acidophilic LysoTracker probe with the *Mtb* phagosomes was observed in TB patients' alveolar macrophages, whether with single or multiple *Mtb* in membrane-bound vacuoles, after *ex vivo* culture for 16–18 h (Fig. 6A). Also, no colocalization of the *Mtb* phagosomes with filamentous actin was identified (Fig. S9A). However, we detected numerous intracellular vesicles containing *Mtb* LAM which were positive for LysoTracker and were surrounded by a cortex of filamentous actin in the same host cells (Fig. 6A, B, and Fig. S9A, B). Therefore, on the one hand, the TB patients' alveolar macrophages retained their function to regulate the vesicle trafficking pathway. However, on the other hand, *Mtb* with different virulence, as single and in large colonies, including those with cording morphology, manipulated vesicular traffic, inhibiting phagolysosomal biogenesis, and avoided host killing in the phagosomes of the TB patients' alveolar macrophages.

4. Discussion

Tuberculosis is a dangerous airborne disease caused by *Mtb* and characterized by a tight interplay between *Mtb* and host cells, mainly alveolar macrophages. Macrophages are the cells of the primary immune response acting to attack and kill infectious agents, including *Mtb*. However, *Mtb* can survive, replicate, and persist in human lungs for a long time [6,8–11,30,31]. Studies of the mechanisms of *Mtb* survival within alveolar macrophages during human TB disease are extremely important for the development of new vaccines and methods for TB treatment. In our study, to locate *Mtb* in the TB patients' and guinea pig' alveolar macrophages in *ex vivo* culture, we used a confocal fluorescent microscopy assay of phagosomal integrity, based on the use of digitonin to label *Mtb* that are in the cytoplasm or within membrane-disrupted phagosomes, and then a light microscopy assay of same macrophages as on the fluorescent images re-stained for acid-fast *Mtb* by the ZN method. Our data indicate that *Mtb* with different virulence, as single and in colonies, including those with cording morphology, are exclusively intravacuolar pathogens with intact phagosomal membranes in alveolar macrophages of all the TB patients and guinea pig with clinical and histopathological signs of TB disease after *ex vivo* culture for 16–20 h. Our results are consistent with the findings of many scientific groups [7,23–25], but differ from several reports that have documented the escape of *Mtb* from phagosomes to the cytoplasm of host cells and increased death rates of these cells usually infected *in vitro* and examined by electron microscopy [13,14] and/or in the FRET image test [15–18] after 2–7 days of infection. Consequently, it was proposed that the translocation of *Mtb* into the cytoplasm led to the induction of host cell death [13,15–18]. In the present study, we found some *Mtb* in the cytoplasm and/or, more likely, damaged vacuoles exclusively in alveolar macrophages with morphological signs of cell death in the cell culture of only one patient after prolonged (5 days) *ex vivo* culture, where many alveolar macrophages with apoptotic or necrotic morphology, with and without *Mtb* in them, were found. Nevertheless, in this *ex vivo* cell culture, we identified *Mtb* inside intact phagosomes in other cells with apoptotic or necrotic morphology. These findings led us to hypothesize that the death of alveolar macrophages precedes the damage of phagosomal membranes and then, probably, the *Mtb* vacuole-to-cytosol translocation, but not vice versa. In the our previous study of BCG mycobacterium-host cell relationships, we had revealed a considerable increase in BCG mycobacteria in the macrophages of mouse bone marrow and peritoneal cell cultures within 5 days following infection with BCG *in vitro* and the death of many cells with increased BCG mycobacterial loads [28]. Here, the causes of the death of alveolar macrophages, with or without *Mtb* that demonstrated a low level of virulence in the guinea pig TB model, remained unknown,

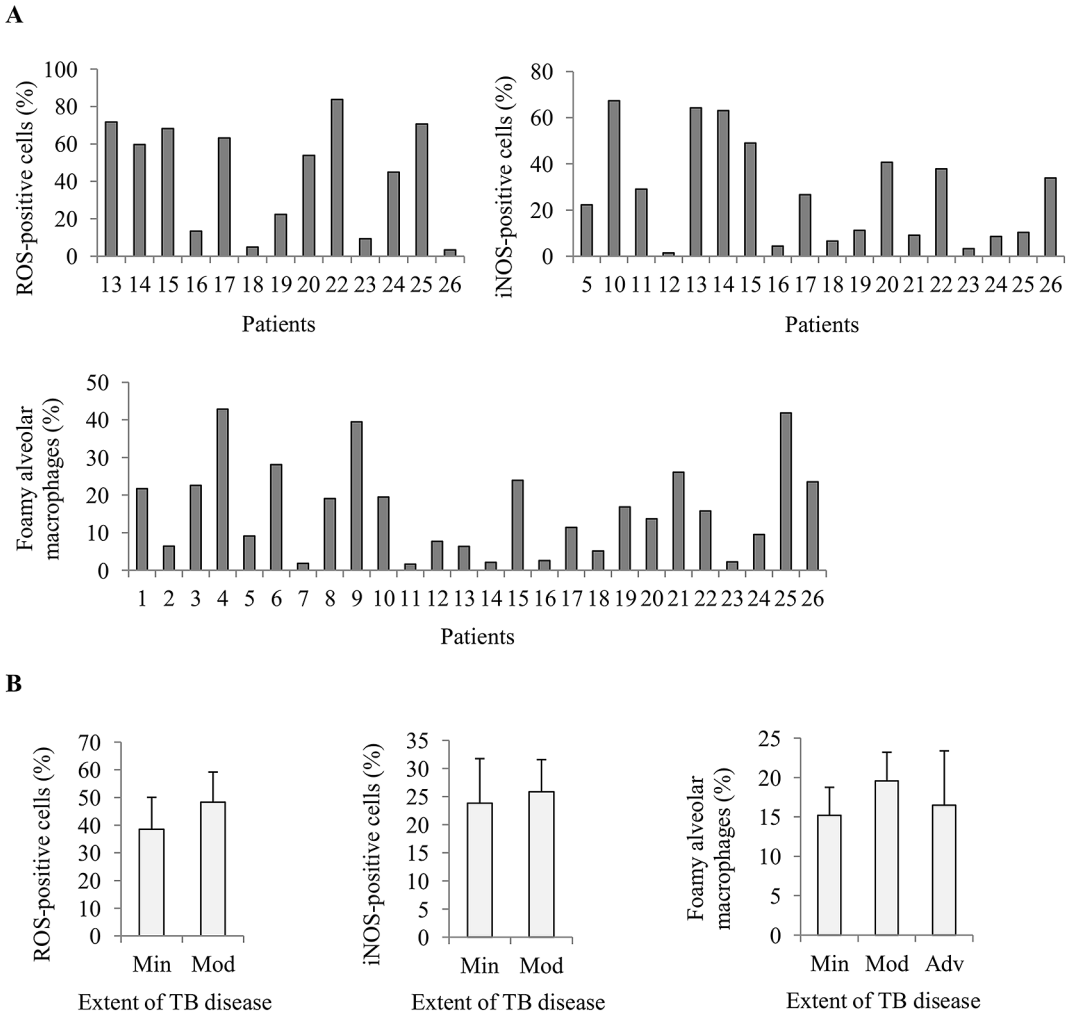

Fig. 5. The number of ROS-positive, iNOS-positive, and foamy alveolar macrophages is different in the *ex vivo* cell cultures of TB patients. (A) The number of alveolar macrophages with human markers expressed as the percentage of the total number of the patients' alveolar macrophages analyzed after *ex vivo* culture for 16–18 h. Alveolar macrophages were considered foamy when more than one-third of the cell surface was stained by the Nile red dye. (B) No difference in the mean population size of alveolar macrophages with human markers was found between the patient groups with the "minimal" (Min; $n_{ROS} = 6$, $n_{iNOS} = 9$, and $n_{foamy} = 14$), "moderate" (Mod; $n_{ROS} = 7$, $n_{iNOS} = 8$, and $n_{foamy} = 8$), and "advanced" (Adv; $n_{foamy} = 3$) extents of TB disease. Data are expressed as the means ± SEM.

because no changes in bacterial load were found in the cell cultures of patient 24 after 18 h and 5 days of *ex vivo* culture. According to David G. Russell [7], *Mtb* escape from its phagosomes into the macrophage cytoplasm may represent a transient and short-time state that could be essential for *Mtb* exit and dissemination under specific host environmental conditions, but the mechanisms of these processes are yet to be studied. Here, *Mtb* with different virulence resided only in the phagosomes of the TB patients' viable alveolar macrophages in all the *ex vivo* cell cultures. Consequently, the intravacuolar localization of *Mtb* is the most favorable niche for its survival and reproduction in colonies, including those with cording morphology, during TB disease.

Note that the FRET assay of *Mtb* vacuole-to-cytosol translocation detects the mixing of phagosomal content with the cytosol, when the presence of β-lactamase activity is determined only on the cell surface of *Mtb* in the absence of the secretion of this enzyme by microbes in host cells, because proteome analyses have identified β-lactamase as a membrane-associated protein containing a lipobox motif in its signal sequence, which predicts its membrane-anchored cell envelope localization [15–18,20,40–42]. However, more research is needed to establish the biogenesis of *Mtb* β-lactamase in host cells, both infected in *in vitro* cell cultures and obtained from the different tissues of TB patients and animals. As is known, the complexity of the host environment during TB disease cannot be reproduced in cell cultures infected *in vitro* and, as has been established by many authors, *Mycobacterium*-host cell relationships in granuloma cells of people and animals with TB disease and cells infected *in vitro* are very different [3,5,6,11,28].

As was previously indicated [13,14,43], the ESX-1 secretion system and ESAT-6 protein were required for the perforation/lysis of phagosomal membranes and *Mtb* escape from the vacuole into the cytoplasm of host cells after infection in *in vitro* cell cultures. In the present study, we identified the ESAT-6 protein and other *Mtb* products in numerous membrane-bound intact vesicles in the TB patients' alveolar macrophages, with or without *Mtb* in them. Additionally, we observed many cells stained for *Mtb* markers (Ag38, ESAT-6, and LAM) and human products on histological sections of the resected lungs of TB patients both with an increased number of *Mtb*-infected alveolar macrophages and with single host cells with *Mtb* in the *ex vivo* cell cultures. By common opinion, large amounts of *Mtb* LAM and other *Mtb* antigens frequently revealed in the bodily fluids (for example, in urine [44,45]), biological clinical samples (for example, BAL fluid [46]), and on antibody-stained histological sections of TB patients' lung tissues without detectable acid-fast *Mtb*, result from a relatively low sensitivity and specificity of the ZN staining [47–49]. However, previously [30] and now, we have determined that the use of the different staining techniques (ZN and Ag38/ESAT-6/LAM immunofluorescent staining) produce similar numbers of alveolar macrophages with *Mtb* in all *ex vivo*

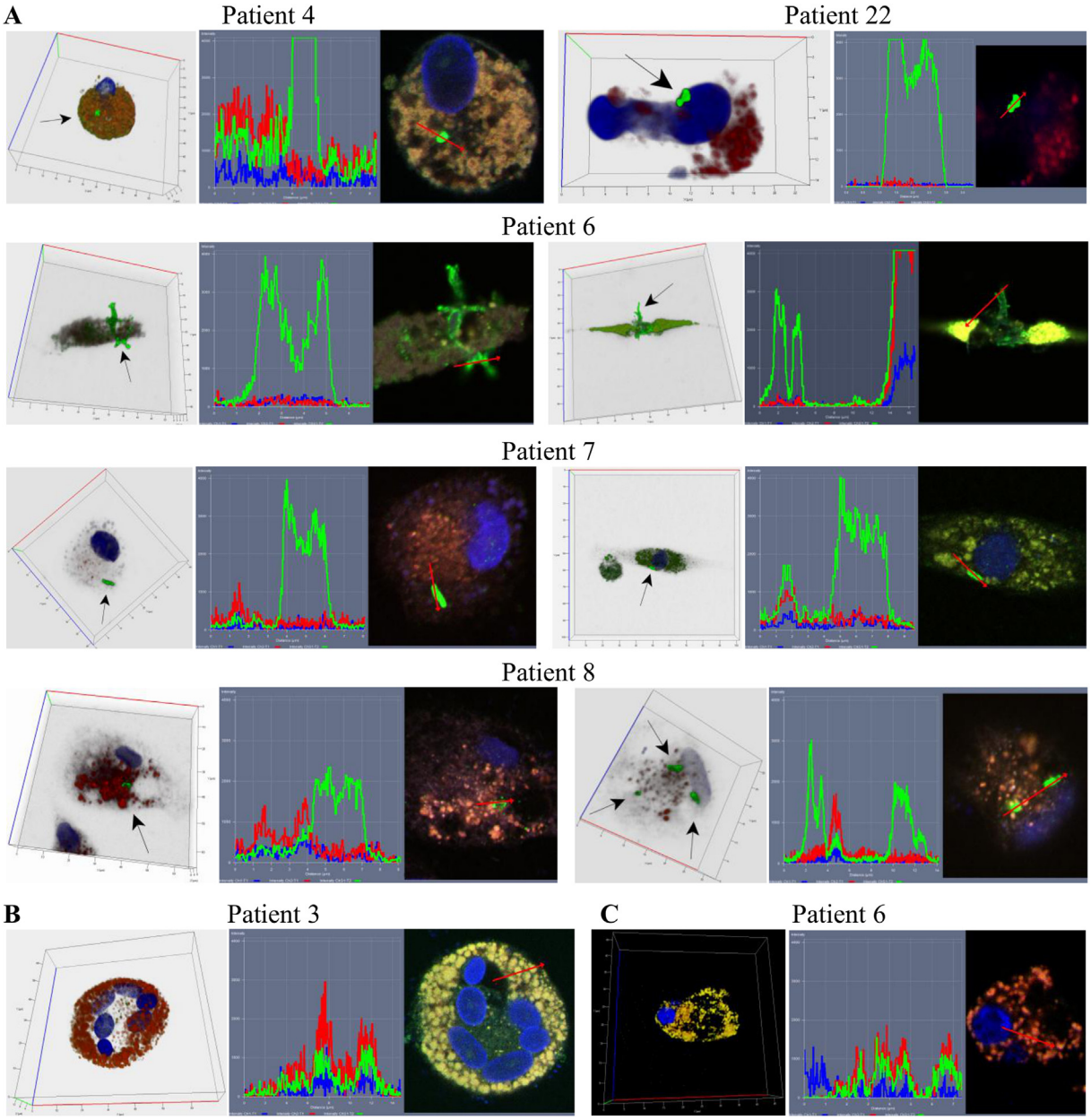

Fig. 6. Mycobacteria avoid delivery to lysosomes in TB patients' alveolar macrophages. (A, B) Representative confocal fluorescent images of cells (after *ex vivo* culture for 16–18 h) stained by *Mtb* LAM-specific antibodies (green signal) and the LysoTracker Red DND-99 dye (red signal) demonstrate lack of colocalization of LAM with host cell lysosomes (lack of yellow signal) in (A) the *Mtb* phagosomes, however (A–B) numerous host cell vesicles with *Mtb* products fused with lysosomes (yellow signal). Nuclei are stained by DAPI (blue signal). (A) Black arrows point to *Mtb* (as single and in colonies, with or without cording) on the 3D images of host cells. (A–C) To the right of the 3D images: the profile images of the *Mtb* phagosomes and human vesicles in these cells. Red arrows define the areas used for constructing profile images. (C) A representative confocal fluorescent image of an alveolar macrophage (after *ex vivo* culture for 18 h) stained by *Mtb* Ag38-specific (green signal) and *Mtb* ESAT-6-specific (red signal) antibodies shows colocalization of these *Mtb* markers (yellow signal) in human vesicles. (For interpretation of the references to colour in this figure legend, the reader is referred to the Web version of this article.)

cell cultures of each TB patient. Together, the original and others' data indicate that *Mtb* antigens are found mainly in the numerous vesicles stained by *Mtb*-specific antibodies both on histological sections of the TB patients' lungs and in the *ex vivo* cultures of the TB patients' alveolar macrophages. Moreover, these *Mtb* products are likely to have been stored in these vesicular compartments for a long time, even when the number of *Mtb*-infected cells in the lungs of the TB patients became very small as a result of TB treatment. We found that intracellular vesicles, too, may contain *Mtb* DNA and/or RNA, probably for a long time, in many alveolar macrophages of the TB patients. Some researchers detected *Mtb* DNA and transcripts of *Mtb* genes in many cells on histological sections of TB patients' lung pieces in the absence of acid-fast *Mtb* in these tissues [50]. Therefore, the use of histochemistry, with the immunostaining and/or *in situ* hybridization for *Mtb* antigens, as a diagnostic tool for identifying the number *Mtb*-infected cells and the characteristics of the *Mtb* population in the lungs of TB patients has limited value in clinical assays because of the predominant visualization of intracellular vesicles with *Mtb* products in human cells on histological sections. Today, only our technique for isolation of alveolar macrophages from the resected lung tissues of patients with pulmonary TB determines rapidly (in two days after surgery) the level of infection with *Mtb* in the cells of the resected lungs and, by the presence or absence of *Mtb* colonies, the functional status of the TB agent, its virulence at the time of surgery [30,31] and, here, addresses intracellular lifestyle

of *Mtb* in human lungs. This information can be used as the basis for the development of individual strategies in post-operative case treatment of patients with pulmonary TB.

In this study, we identified *Mtb* within intact phagosomes with the different signs: the presence of the receptor CD14 and ROS, iNOS, lipids or the lack of these antimicrobial agents and sources of nutrients and energy, - in the TB patients' alveolar macrophages. No colocalization of LAM-labeled *Mtb* (with different virulence, as single and in colonies, including those with cording morphology) with acidic compartments positive for LysoTracker dye or filamentous actin was observed in these cells of all the TB patients. However, it was determined that LAM-containing vesicles fused with lysosomes in host cells with *Mtb* and were surrounded by a cortex of filamentous actin, which is important for endosome processing, vacuolar intracellular transport and fusions along the endosomal pathway [9]. While the lack of fusion of the *Mtb* phagosomes with the acidophilic fluorescent LysoTracker probe and, consequently, lysosomes has been pointed out by many researchers who has been studying *Mtb*-contained cells infected in *in vitro* cell cultures [4,51,52] and during our study of granuloma macrophages isolated from mice with latent TB infection [27,28], here we have found that this phenomenon is also observed in TB patients' alveolar macrophages with different numbers of *Mtb*, as single and in colonies, including those with cording morphology. This result is consistent with the data obtained in the study of BAL cells from patients with pulmonary TB examined by immunoelectron microscopy [23]. In our work, we also found that the normal process of endosome-to-endolysosome maturation and trafficking pathways of vesicles containing *Mtb* markers are maintained in the same host cells with the *Mtb* phagosomes in them. In addition, we have determined that the *Mtb* phagosomes interact with human different endocytic pathways, for the presence of the receptor CD14, iNOS, ROS, and lipids in them, in TB patients' alveolar macrophages, even though they avoid fusion with lysosomes and filamentous actin. Thus, the arrest of the biogenesis of phagolysosomes with *Mtb* in TB patients' alveolar macrophages is not defined only by the presence of LAM, Ag38, and/or ESAT-6 in these intracellular compartments, as was previously thought [4,5]. No accumulation of *Mtb* LAM on the cytoplasmic side of the *Mtb* phagosomes was found in the TB patients' alveolar macrophages, therefore the activity of this *Mtb* factor was not thought to interfere with the effects of phosphatidylinositol 3-phosphate on the phagosomal membrane and, consequently, to modulate the recruitment of the vacuolar GTPases to the *Mtb* phagosome [4,6,39,53,54]. Overall, further research is required to elucidate the molecular mechanisms involved in the inhibition of *Mtb* phagolysosomal biogenesis, because the arrest of phagosome-to-phagolysosome maturation is the key mechanism by which *Mtb* avoid host killing and survive within host cells, including alveolar macrophages of patients with pulmonary TB.

5. Conclusion

In this study, we have developed the *ex vivo* cultures of alveolar macrophages obtained from the resected lung tissues of patients with pulmonary TB to establish the unique features of *Mtb* lifestyle in human lung cells. The strategy used allowed us to learn that intact membrane-bound compartments are the primary intracellular niche for *Mtb* in TB patients' alveolar macrophages, where *Mtb* with different virulence survive and replicate in colonies, including those with cording morphology, during human TB disease. The results described here also indicate that the *Mtb* phagosomes are not the isolated organelles in the TB patients' alveolar macrophages, but entities dynamically interacting with the host endosomal system and communicating with the host molecular machineries, such as CD14, ROS, iNOS, and lipids, yet avoiding fusion with host lysosomes. Finally, our findings provide a crucial insight into *Mtb* pathogenesis during human TB disease. Understanding how *Mtb* survive within host cells and manipulate host signaling pathways is very important both for identification of novel therapeutic and pharmacological targets to combat TB disease, including the development of host-directed therapies to fight *Mtb* infection, and for the comprehension of fundamental eukaryotic and microbial cellular processes.

Conflicts of interest

The authors declare that they have no competing interests.

Acknowledgments

The authors are thankful to T. Aleshina (Shared Center for Microscopic Analysis of Biological Objects of the Institute of Cytology and Genetics, Novosibirsk) for technical support, S. Karskanova and E. Petrunina (Ural Research Institute for Phthisiopulmonology, Yekaterinburg) for help with testing TB patients.

Appendix A. Supplementary data

Supplementary data to this article can be found online at https://doi.org/10.1016/j.tube.2018.12.002.

References

[1] Kyu HH, Maddison ER, Henry NJ, Mumford JE, Barber R, Shields C, et al. The global burden of tuberculosis: results from the global burden of disease study 2015. Lancet Infect Dis 2018;18:261–84. https://doi.org/10.1016/S1473-3099(17)30703-X.
[2] World Health Organization. Drug-resistant TB: surveillance and response. Supplement to Global tuberculosis report 2014. Geneva, Switzerland: WHO; 2014.
[3] Smith I. *Mycobacterium tuberculosis* pathogenesis and molecular determinants of virulence. Clin Microbiol Rev 2003;16:463–96. https://doi.org/10.1128/CMR.16.3.463–496.2003.
[4] Vergne I, Chua J, Singh SB, Deretic V. Cell biology of *Mycobacterium tuberculosis* phagosome. Annu Rev Cell Dev Biol 2004;20:367–94. https://doi.org/10.1146/annurev.cellbio.20.010403.114015.
[5] Uribe-Querol E, Rosales C. Control of phagocytosis by microbial pathogens. Front Immunol 2017;8:1368. https://doi.org/10.3389/fimmu.2017.01368.
[6] Guirado E, Schlesinger LS, Kaplan G. Macrophages in tuberculosis: friend or foe. Semin Immunopathol 2013;35:563–83. https://doi.org/10.1007/s00281-013-0388-2.
[7] Russell DG. The ins and outs of the *Mycobacterium tuberculosis*-containing vacuole. Cell Microbiol 2016;18:1065–9. https://doi.org/10.1111/cmi.12623.
[8] Welin A, Winberg ME, Abdalla H, Särndahl E, Rasmusson B, Stendahl O, et al. Incorporation of *Mycobacterium tuberculosis* lipoarabinomannan into macrophage membrane rafts is a prerequisite for the phagosomal maturation block. Infect Immun 2008;76:2882–7. https://doi.org/10.1128/IAI.01549-07.
[9] Anes E. For host factors weddings and a Koch's bacillus funeral: actin, lipids, phagosome maturation and inflammasome activation. In: Cardona P-J, editor. Understanding tuberculosis – analyzing the origin of *Mycobacterium tuberculosis* pathogenicity. Vienna: InTech; 2012. p. 123–48.
[10] Källenius G, Correia-Neves M, Buteme H, Hamasur B, Svenson SB. Lipoarabinomannan, and its related glycolipids, induce divergent and opposing immune responses to *Mycobacterium tuberculosis* depending on structural diversity and experimental variations. Tuberculosis 2016;96:120–30. https://doi.org/10.1016/j.tube.2015.09.005.
[11] Espitia C, Rodriguez E, Ramyn-Luing L, Echeverria-Valencia G, Vallecillo AJ. Host–pathogen interactions in tuberculosis. In: Cardona P-J, editor. Understanding tuberculosis – analyzing the origin of *Mycobacterium tuberculosis* pathogenicity. Vienna: InTech; 2012. p. 43–76.
[12] Forrellad MA, Klepp LI, Gioffré A, Sabio y García J, Morbidoni HR, de la Paz Santangelo M, et al. Virulence factors of the *Mycobacterium tuberculosis* complex. Virulence 2013;4:3–66. https://doi.org/10.4161/viru.22329.
[13] van der Wel N, Hava D, Houben D, Fluitsma D, van Zon M, Pierson J, et al. *M. tuberculosis* and *M. leprae* translocate from the phagolysosome to the cytosol in myeloid cells. Cell 2007;129:1287–98. https://doi.org/10.1016/j.cell.2007.05.059.
[14] Houben D, Demangel C, van Ingen J, Perez J, Baldeón L, Abdallah Abdallah M, et al. ESX-1-mediated translocation to the cytosol controls virulence of mycobacteria. Cell Microbiol 2012;14:1287–98. https://doi.org/10.1111/j.1462-5822.2012.01799.x.
[15] Simeone R, Bobard A, Lippmann J, Bitter W, Majlessi L, Brosch R, Enninga J. Phagosomal rupture by *Mycobacterium tuberculosis* results in toxicity and host cell death. PLoS Pathog 2012;8. https://doi.org/10.1371/journal.ppat.1002507. e1002507.
[16] Simeone R, Sayes F, Song O, Gröschel MI, Brodin P, Brosch R, Majlessi L. Cytosolic access of *Mycobacterium tuberculosis*: critical impact of phagosomal acidification control and demonstration of occurrence *in vivo*. PLoS Pathog 2015;10. https://doi.org/10.1371/journal.ppat.1004650. e1004650.
[17] Srinivasan L, Gurses SA, Hurley BE, Miller JL, Karakousis PC, Briken V.

Identification of a transcription factor that regulates host cell exit and virulence of *Mycobacterium tuberculosis*. PLoS Pathog 2016;12. https://doi.org/10.1371/journal.ppat.100565. e1005652.
[18] Quigley J, Hughitt VK, Velikovsky CA, Mariuzza RA, El-Sayed NM, Briken V. The cell wall lipid PDIM contributes to phagosomal escape and host cell exit of *Mycobacterium tuberculosis*. mBio 2017;8. https://doi.org/10.1128/mBio.00148-17. e00148-00117.
[19] Ray K, Bobard A, Danckaert A, Paz-Haftel I, Clair C, Ehsani S, et al. Tracking the dynamic interplay between bacterial and host factors during pathogen-induced vacuole rupture in real time. Cell Microbiol 2010;12:545–56. https://doi.org/10.1111/j.1462-5822.2010.01428.x.
[20] Kurz SG, Bonomo RA. Reappraising the use of β-lactams to treat tuberculosis. Expert Rev Anti Infect Ther 2012;10:999–1006. https://doi.org/10.1586/eri.12.96.
[21] Simeone R, Majlessi L, Enninga J, Brosch R. Perspectives on mycobacterial vacuole-to-cytosol translocation: the importance of cytosolic access. Cell Microbiol 2016;18:1070–7. https://doi.org/10.1111/cmi.12622.
[22] Queval CJ, Brosch R, Simeone R. The macrophage: a disputed fortress in the battle against *Mycobacterium tuberculosis*. Front Microbiol 2017;8:2284. https://doi.org/10.3389/fmicb.2017.02284.
[23] Mwandumba HC, Russell DG, Nyirenda MH, Anderson J, White SA, Molyneux ME, et al. *Mycobacterium tuberculosis* resides in nonacidified vacuoles in endocytically competent alveolar macrophages from patients with tuberculosis and HIV infection. J Immunol 2004;172:4592–8. https://doi.org/10.4049/jimmunol.172.7.4592.
[24] Harriff MJ, Purdy GE, Lewinsohn DM. Escape from the phagosome: the explanation for MHC-I processing of mycobacterial antigens? Front Immunol 2012;3:40. https://doi.org/10.3389/fimmu.2012.00040.
[25] Harriff MJ, Cansler ME, Toren KG, Canfield ET, Kwak S, Gold MC, et al. Human lung epithelial cells contain *Mycobacterium tuberculosis* in a late endosomal vacuole and are efficiently recognized by CD8(+) T cells. PloS One 2014;9:e97515https://doi.org/10.1371/journal.pone.0097515.
[26] Ufimtseva E. Investigation of functional activity of cells in granulomatous inflammatory lesions from mice with latent tuberculous infection in the new *ex vivo* model. Clin Dev Immunol 2013;2013. https://doi.org/10.1155/2013/371249. ID371249.
[27] Ufimtseva E. *Mycobacterium*-host cell relationships in granulomatous lesions in a mouse model of latent tuberculous infection. BioMed Res Int 2015;2015. https://doi.org/10.1155/2015/948131. ID 948131.
[28] Ufimtseva E. Differences between *Mycobacterium*-host cell relationships in latent tuberculous infection of mice *ex vivo* and mycobacterial infection of mouse cells *in vitro*. J Immunol Res 2016;2016. https://doi.org/10.1155/2016/4325646. ID 4325646.
[29] Ufimtseva E. The control of apoptotic death in the cells of granulomatous inflammatory lesions from mice with latent tuberculous infection in the *ex vivo* model. Immunome Res 2017;13:128. https://doi.org/10.4172/17457580.1000128.
[30] Ufimtseva E, Eremeeva N, Petrunina E, Umpeleva T, Karskanova S, Baiborodin S, et al. *Ex vivo* expansion of alveolar macrophages with *Mycobacterium tuberculosis* from the resected lungs of patients with pulmonary tuberculosis. PloS One 2018;13. https://doi.org/10.1371/journal.pone.019191. e0191918.
[31] Ufimtseva EG, Eremeeva NI, Petrunina EM, Umpeleva TV, Baiborodin SI, Vakhrusheva DV, et al. *Mycobacterium tuberculosis* cording in alveolar macrophages of patients with pulmonary tuberculosis is likely associated with increased mycobacterial virulence. Tuberculosis 2018;112:1–10. https://doi.org/10.1016/j.tube.2018.07.001.
[32] Checroun C, Wehrly TD, Fischer ER, Hayes SF, Celli J. Autophagy-mediated reentry of *Francisella tularensis* into the endocytic compartment after cytoplasmic replication. Proc Natl Acad Sci USA 2006;103:14578–83. https://doi.org/10.1073/pnas.0601838103.
[33] Collins CA, De Mazière A, van Dijk S, Carlsson F, Klumperman J, Brown EJ. Atg5-independent sequestration of ubiquitinated mycobacteria. PLoS Pathog 2009;5. https://doi.org/10.1371/journal.ppat.1000430. e1000430.
[34] Ufimtseva EG, Eremeeva NI, Kravchenko MI, Skornyakov SN. Method for producing ex vivo alveolar macrophage cultures of the operational material of patients suffering pulmonary tuberculosis and method for estimating virulence of Mycobacterium tuberculosis using the obtained ex vivo alveolar macrophage cultures. RF Patent RU2593725. Bull Izobr 2016;22:1–30.
[35] Eremeeva NI, Vakhrusheva DV, Kravchenko MA, Kanischev VV, Umpeleva TV, Belousova KV, et al. Monitoring of MBT contamination of environment of health organization. Ptisiatria Pulmonol (Russia) 2016;1:102–19.
[36] Ufimtseva EG, Eremeeva NI, Kravchenko MI, Skornyakov SN. Method for determining the ability of Mycobacteria of tuberculosis to growth in alveolar macrophages of patients after the course of antituberculosis therapy. RF Patent RU2652882. Bull Izobr 2018;13:1–20.
[37] Uvarova EA, Belavin PA, Permyakova NV, Zagorskaya AA, Nosareva OV, Kakimzhanova AA, et al. Oral immunogenicity of plant-made *Mycobacterium tuberculosis* ESAT6 and CFP10. BioMed Res Int 2013;2013. https://doi.org/10.1155/2013/316304. ID316304.
[38] van Loo G, Saelens X, van Gurp M, MacFarlane M, Martin SJ, Vandenabeele P. The role of mitochondrial factors in apoptosis: a Russian roulette with more than one bullet. Cell Death Differ 2002;9:1031–42. https://doi.org/10.1038/sj.cdd.4401088.
[39] Ashkenazi A, Fairbrother WJ, Leverson JD, Souers AJ. From basic apoptosis discoveries to advanced selective BCL-2 family inhibitors. Nat Rev Drug Discov 2017;16:273–84. https://doi.org/10.1038/nrd.2016.253.
[40] Målen H, Pathak S, Søfteland T, de Souza GA, Wiker HG. Definition of novel cell envelope associated proteins in Triton X-114 extracts of *Mycobacterium tuberculosis* H37Rv. BMC Microbiol 2010;10. https://doi.org/10.1186/1471-2180-10-132. 132-132.
[41] Maffei B, Francetic O, Subtil A. Tracking proteins secreted by bacteria: what's in the toolbox? Front Cell Infect Microbiol 2017;7:221. https://doi.org/10.3389/fcimb.2017.00221.
[42] Perkowski EF, Zulauf KE, Weerakoon D, Hayden JD, Ioerger TR, Oreper D, et al. The EXIT strategy: an approach for identifying bacterial proteins exported during host infection. mBio 2017;8. https://doi.org/10.1128/mBio. e00333-17.
[43] Manzanillo PS, Shiloh MU, Portnoy DA, Cox JS. Mycobacterium tuberculosis activates the DNA-dependent cytosolic surveillance pathway within macrophages. Cell Host Microbe 2012;11:469–80. https://doi.org/10.1016/j.chom.2012.03.007.
[44] Gupta-Wright A, Peters JA, Flach C, Lawn SD. Detection of lipoarabinomannan (LAM) in urine is an independent predictor of mortality risk in patients receiving treatment for HIV-associated tuberculosis in sub-Saharan Africa: a systematic review and meta-analysis. BMC Med 2016;14:53. https://doi.org/10.1186/s12916-016-0603-9.
[45] Lawn SD, Gupta-Wright A. Detection of lipoarabinomannan (LAM) in urine is indicative of disseminated TB with renal involvement in patients living with HIV and advanced immunodeficiency: evidence and implications. Trans R Soc Trop Med Hyg 2016;110:180–5. https://doi.org/10.1093/trstmh/trw008.
[46] Kruh-Garcia NA, Schorey JS, Dobos KM. Exosomes: new tuberculosis biomarkers – prospects from the bench to the clinic. In: Cardona P-J, editor. Understanding tuberculosis – global experiences and innovative approaches to the diagnosis. Vienna: InTech; 2012. p. 395–410.
[47] Hunter RL, Actor JK, Hwang S-A, Karev V, Jagannath C. Pathogenesis of post primary tuberculosis: immunity and hypersensitivity in the development of cavities. Ann Clin Lab Sci 2014;44:365–87.
[48] Karimi S, Shamaei M, Pourabdollah M, Sadr M, Karbasi M, Kiani A, et al. Histopathological findings in immunohistological staining of the granulomatous tissue reaction associated with tuberculosis. Tuberc Res Treat 2014;2014:6. https://doi.org/10.1155/2014/858396.
[49] Mustafa T, Leversen NA, Sviland L, Wiker HG. Differential *in vivo* expression of mycobacterial antigens in *Mycobacterium tuberculosis* infected lungs and lymph node tissues. BMC Infect Dis 2014;14:535. https://doi.org/10.1186/1471-2334-14-535.
[50] Fenhalls G, Stevens L, Moses L, Bezuidenhout J, Betts JC, Helden PV, et al. In situ detection of *Mycobacterium tuberculosis* transcripts in human lung granulomas reveals differential gene expression in necrotic lesions. Infect Immun 2002;70:6330–8. https://doi.org/10.1128/IAI.70.11.6330–6338.2002.
[51] Via LE, Fratti RA, McFalone M, Pagan-Ramos E, Deretic D, Deretic V. Effects of cytokines on mycobacterial phagosome maturation. J Cell Sci 1998;111:897–905.
[52] Tailleux L, Neyrolles O, Honoré-Bouakline S, Perret E, Sanchez F, Abastado J-P, et al. Constrained intracellular survival of Mycobacterium tuberculosis in human dendritic cells. J Immunol 2003;170:1939–48. https://doi.org/10.4049/jimmunol.170.4.1939.
[53] López de Armentia MM, Amaya C, Colombo MI. Rab GTPases and the autophagy pathway: bacterial targets for a suitable biogenesis and trafficking of their own vacuoles. Cells 2016;5:11. https://doi.org/10.3390/cells5010011.
[54] Prashar A, Schnettger L, Bernard EM, Gutierrez MG. Rab GTPases in immunity and inflammation. Front Cell Infect Microbiol 2017;7:435. https://doi.org/10.3389/fcimb.2017.00435.